

Modeling of the Spread of an Effluent and the Overturning Length Scale near an Underwater Source in the Northern Adriatic

Vlado Malačič* and Patricija Mozetič

Marine Biology Station, National Institute of Biology, Piran, Slovenia

Received May 18, 2005

INTRODUCTION

The spread of sewage in a coastal sea is a complex phenomenon that includes mechanisms that act on different environmental scales. In this work, a review of different mechanisms will be presented, all mostly confined to the hydrodynamic conditions of sewage that leaves a treatment plant and travels to the sea through sewage pipes (first stage), spreads into the sea through the diffuser orifices in cone-like structures (second stage, initial dilution), forms a patch of pollutant around the source (third stage), and dilutes further with the motion of ambient fluid, through turbulent diffusion and advection, that stretches the initial patch (fourth stage, secondary dilution). This process is also called turbulent dispersion, in which mixing and dilution take place.¹ In a study of the spread of sewage from two submarine diffusers off the town of Piran and from a single diffuser off the town of Izola (see Figure 1 for locations), the sewage near field was surveyed with a conductivity, temperature, and depth (CTD) probe in a very shallow sea (depths less than 21 m). The hydraulics of the discharge system were also studied,² because the flow rates and buoyancy fluxes through the orifices of the diffusers are the initial conditions for the modeling of the initial dilution of sewage in the sea.³ A review will be presented of numerical solutions of the dilution of the initial phase, when a conservative pollutant is rising toward a layer of neutral buoyancy. This process takes place on a scale of 20 m. Formation of the initial patch of effluent above the sewage diffusers will be estimated through the space distribution of the overturning length scale on a slightly larger scale (up to 500 m). Secondary dilution, which mainly depends on advection, will also be examined for a specific, yet typical, case of wind-driven circulation when it is supposed that the effluent reaches the surface layer, if released outside the Bay of Koper near the center of the Gulf of Trieste. It is supposed that, during the initial dilution, the pollutant is a conservative one, since this process takes less than 1 min, while in the case of secondary dilution, a decay of faecal coliforms on a time scale of hours is supposed.

Small wiggles on the vertical profiles of temperature and salinity were observed on vertical CTD profiles in a near field above the submarine source of sewage. They resulted in small wiggles on the vertical profiles of density. Many of them could not be explained simply by temperature and conductivity mismatches due to the different dynamic responses of the probes.⁴ It is suspected, however, that they

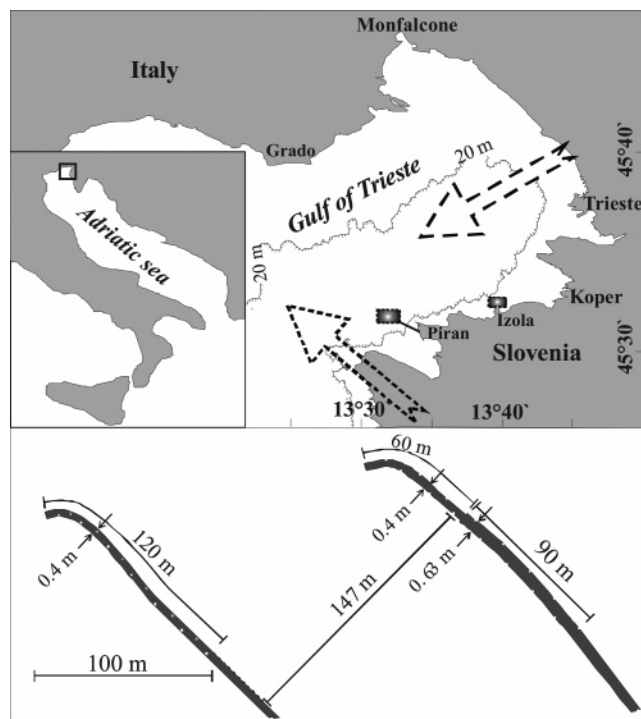


Figure 1. Top: Location map of the sewage outfall off Piran composed of two pipes that end with diffusers above which the near field was explored (larger dashed rectangle) and an outflow of another small town (Izola) little more than 200 m offshore that was also surveyed (smaller rectangle). The dotted arrow represents the Sirocco (Jugo) wind that blows along the axis of the Adriatic Sea, while the Bora (Burja) wind (dashed arrow) blows along the axis of the Gulf of Trieste. Bottom: two parallel pipelines of the outfall off Piran that end with diffusers, which were deflected westward at the time of the CTD surveys (1996–1998). Diffusers are 2.6 km away from the nearest land point.

are related to the presence of a turbulent sewage fluid, already mixed with the surrounding water, that is spreading horizontally at a level of neutral buoyancy. The detection of sewage that may spread horizontally in a layer that is less than 0.5-m-thick is a key problem in field observations when its depth is not known in advance. There are numerous mechanisms that cause these small vertical fluctuations of density, such as internal waves⁵ with their breaking, surface wave breaking,⁶ wind-driven Langmuir cells over the ocean,⁷ patchy turbulent mixing at the thermocline,⁸ slope turbulent gravity currents and episodic convective plumes,⁹ surface cooling and convection overturns,¹⁰ and intrusions and underflows of a denser river fluid.¹¹ Different turbulent processes at the sea surface expand deeper into a water column,¹² and a shallow sea may be filled with them. Most

* Corresponding author. E-mail: malacic@mbss.org.

of the time, there is an overlapping of different processes that play a role above the source of sewage, and sometimes, it is hard to distinguish among them.

There have been attempts to look at the links between different properties of seawater. An analysis of water samples showed that, out of eight different nutrient compounds, only ammonium followed the increase of bacteria¹³ with a correlation factor of 0.58. There was no significant correlation between bacteria and fluorescence, nor with dissolved oxygen. Fluorescence measurements showed a patchy distribution of chlorophyll *a* above the diffusers during the winter period¹⁴ when the water column was almost homogeneous. The fluorescence signal is not a distinctive one for the sewage discharged from the outfall at Piran, nor are those of dissolved oxygen or PAR (photosynthetic active radiation), contrary to what has been observed for other much larger outfalls.^{15,16} Methods using a dye, like rhodamine,¹⁷ have not been applied here.

Field campaigns revealed that a layer in which sewage spreads horizontally could hardly be traced with a conventional CTD, without a dye release or a time-consuming sampling technique to analyze the near field for chemical substances (ammonium). The need for quick detection of this layer with a simple CTD cast emerged. For this reason, past CTD surveys were reviewed again in order to apply the overturning length scale (L_T), first introduced in the 1970s.¹⁸ This quantity measures the vertical extent of the overturning vortices that would be required by water parcels in order to find their statically stable position. It was later shown⁵ that L_T is proportional to the Ozmidov length scale $L_o = (\epsilon/N^3)^{1/2}$, where ϵ is the dissipation rate of kinetic energy and N is the buoyancy frequency near the surface in the wind-driven mixed layer. The Ozmidov scale measures the thickness of a fluid in which the buoyancy force is balanced by the inertial force. Dillon⁵ found a match between the two scales ($L_o = 0.8L_T$) that holds well for nearly 3 orders of magnitude in the ocean, as well as in lakes at the base of the mixing layer and thermocline. Both Thorpe¹⁸ and Dillon calculated the overturning length scale from the vertical profiles of temperature.

The evolution and collapse of a turbulent blob was studied in the laboratory,^{19,20} where the maximum thickness of a blob of neutral buoyancy that emerged horizontally in a stratified fluid is proportional to L_T . It seems that there are no applications of the overturning length scale in studies of the spread of turbulent jets in a natural ambient. Density fluctuations obtained in the laboratory are, however, similar to those observed in the sea above the sewage diffusers.

In this work, model results of initial dilution under real stratified conditions in the sea²¹ will be reviewed. They are applied to predict the height above the diffusers of the municipal outfall of Piran where faecal coliforms spread horizontally in a coastal sea. We will not enter into an analysis of the complex formation of a patch that occurs between the primary and secondary dilution, which is elsewhere described for specific cases.²² However, we will present the distribution of the overturning length scale above diffusers, which is a measure of higher turbulence intensity and which can serve as an indication of the near field with a formed patch of a pollutant in alien turbulent water.

From this perspective, new results from a survey above the diffuser of another small town (Izola), which is 200 m

offshore, will be added to a review of past results. Finally, a specific case of secondary dilution in the Gulf of Trieste will be surveyed,³ which illustrates the spread of sewage which is concentrated at the surface and is swept away from the source by the variable wind field. In a discussion, the poor effect of tides will be addressed. New circulation findings under steady wind conditions will be framed in a discussion about the secondary dilution of pollutants in the Gulf of Trieste.

ENVIRONMENTAL CONDITIONS

There are two sewage near fields in the southern part of the Gulf of Trieste (Figure 1) that were surveyed around submarine outfalls. The larger one is around the end of two submarine pipes off the town of Piran. The sea there is reasonably flat, and its depth varies with tides between 20.5 and 21.5 m. The sewage discharge of this town makes up only 7% of the sewage load that arrives in the Gulf of Trieste,²³ with a flow rate that varies from 70 to 130 L/s. Two pipelines of more than 3 km in length and internal diameters of 0.59 and 0.375 m are laid 1 m above the sea floor. The diffusers have orifices with a diameter of 0.1 m on their alternate sides every 10 m. Modeling of the initial dilution entailed a preliminary numerical analysis of diffuser hydraulics in order to estimate sewage flux through individual diffuser orifices.² The pipes carry sewage that has been treated mechanically (screening and removal of sand and grease) and oxygenized.

The second location is around a smaller discharge off the town of Izola. It is found about 200 m from the shoreline and represents only about 6% of the sewage load in the Gulf of Trieste. This system is poor in mechanical dilution, and the flow rate is very unsteady (with a mean flow rate of 70 L/s), not so much because of the diurnal variations of the sewage load but because of its design. Domestic and industrial wastes are collected in a treatment basin where only rough mechanical purification (screening by 1-cm rake) is carried out, while sand and grass removal are not functioning properly. The pumps that push the sewage to the sea are triggered when the sewage in the collecting basin reaches a critical level and function just for a few minutes until the level of a pollutant reaches a second, lower critical level. Since the effluent emerges in the sea in short bursts and has been observed visually to reach the surface layer even when the sea is vertically stratified, this leads to the conclusion that the diffuser's design can hardly match the discharge regime. Because of the transient nature of this source, the hydraulic analysis was not performed. Fortunately, it will soon be out of commission since the town of Izola will redirect its sewage toward a new treatment plant in the neighboring town of Koper (10% of the sewage load). The case of a spread of sewage that would emerge from a potential underwater diffuser in front of the Bay of Koper will be presented.

The most frequent winds are the "Bora" (or "Burja") wind (ENE) and the "Sirocco" or "Jugo" (SE) wind (Figure 1). The Bora wind is more frequent during the winter period and is more gusty and energetic (monthly mean speed of 5.0 m/s) than the Jugo, which has a monthly mean speed between 3.0 and 4.4 m/s.²⁴ During the passage of a cyclone over the Adriatic from west to east, first, a Jugo (more humid) wind blows, which then turns rapidly to a dry Bora wind.

Tides are of a mixed type, represented by seven constituents, four semidiurnal and three diurnal ones, and their nature was studied intensively.^{25,26} Tidal currents mostly follow a standing wave regime, being strong when the rate of sea-surface elevation change is extreme and weak when the elevation is at local extrema. Currents are of an amplitude of 0.1 m/s during spring tides, when the tidal range is 1 m.²⁷ Field work was conducted during the period of slack tides over less than 2 h.

Three field surveys above sewage diffusers will be presented. The first two will be reviews, while the third one will be described for the first time. During the first survey on the morning of September 26, 1997, the weather was windy above the diffusers at Piran; forced mixing and convection was supported by the cold Bora (ENE) wind that had been blowing for several days before the cruise, as it also was during that day. During the few hours of the field survey, instantaneous wind speed ranged between 6 and 11 m/s. The second survey was conducted on a cloudy morning, October 12, 1998, in calm weather conditions, when the southern wind was of a speed lower than 3.0 m/s. The previous 2 weeks had been rainy, and there was a strong autumn peak of several rivers discharging into the northern Adriatic, creating a pool of fresher water at the sea surface. The abundance of faecal coliform bacteria measured at the outlet of the treatment basin a few hours before both field surveys took place ranged from 3.3×10^6 to 8.0×10^6 bacteria/100 mL. The third survey was conducted in clement weather above the discharge from the town of Izola on the morning of May 10, 2000. In this case, the input load from the small collecting basin was estimated to be around 5.3×10^6 faecal coliforms/100 mL.

We estimated the flux of sewage from a single side orifice of a diameter of 0.1 m of the diffuser during the first two field surveys,²¹ which yielded, for the outflow velocity through an orifice, a value of 0.45 ± 0.09 m/s for the first survey and 0.8 ± 0.2 m/s for the second survey. This is an important input parameter in a model of the initial dilution of effluent that spreads in an environment with a known vertical density profile. The Reynolds number Re of a jet near an orifice is, therefore, around 5×10^4 ($Re = u_0 d/\nu$, where the outflow velocity averaged over the orifice's surface $u_0 = 0.5$ m/s, the diameter of the orifice $d = 0.1$ m, and $\nu = 10^{-6}$ m²/s is the kinematic viscosity). The density of an effluent at the place of discharge does not vary much, and we may reasonably suppose for it a constant value of 1000 kg/m³ in both surveys. Major variations are those of the ambient density ρ_a . Since there were serious difficulties estimating the flow rate during pulsed outflow through a single orifice of the diffuser off the town of Izola, the calculation of initial dilution was not performed for the third survey.

METHODS

A. CTD Probe and Surveys. The surveys above the diffusers were composed of vertical profiles of temperature and salinity (density) and were conducted using a CTD probe (see Figure 2). The fine-scale CTD probe that also measures dissolved oxygen and fluorescence was designed by the University of Western Australia for ecological field work. This free-falling CTD probe gives a finer vertical resolution of the temperature and salinity structure of the water column



Figure 2. Free-falling fine-scale FPS2 probe. The probe's weight is 35 kg in air, and it is about 1 m in height. Buoyant floats on top surround the electronics in the cylinder below, which has a pump on the left-hand side that drives the water through the conductivity and oxygen probe. The probe carries the Seabird sensors of temperature (SBE 3-01/F), conductivity (SBE 4-01/O), and oxygen (SBE-13 with Beckman polarographic element), a Digiquartz 0–60 m pressure sensor (with a resolution of 2 mm), and a Minitracka fluorometer from Chelsea Instruments.

than most standard probes.²⁸ The nominal speed of falling is around 1 m/s. However, the final vertical speed of the probe is reached at depths between 4 and 5 m because of inertia, regardless of the stratification. The sampling period of all parameters that are measured is 50 Hz, which provides an average vertical space resolution of a CTD profile of at least 2.5 cm. The accuracy of the pressure sensor is around 2×10^{-3} m (Paroscientific Digiquartz sensor, depth 0–60 m). Each cast lasts for less than 25 s (for depths shallower than 22 m). It is estimated that the horizontal drift of the probe (vessel) within this time is much less than 25 m under a wind speed below 6 m/s.

The surveys above the diffusers were composed of a net of CTD stations that were separated by 0.1' (185 m) in the S–N direction and 0.1' (130 m) in the E–W direction. Above the diffusers off Piran, the depth is around 21 m, while above the diffuser at Izola, it is around 12 m. Therefore, 31 stations were chosen for the survey above the diffusers off Piran, while the new survey around the diffuser off Izola near the coastline was composed of only 11 stations. The vessel was positioned at each station using the global positioning system. The position resolution was then estimated to be around 35 m by following the fluctuations of position on several occasions. The vessel stayed at each station for about 3–7 min and was not anchored. Since anchoring is prohibited at these places, the discrepancy between the idealized net of stations and the actual ones is quite pronounced in heavier wind weather, as is seen from the distribution of stations (Figure 3, top left). In the first two cases, the time for the survey was less than 2.5 h, while for the last, it was less than 1 h.

At the central CTD station, after the completion of a CTD survey, samples for bacterial analysis were taken. At depths where small-scale wiggles were detected in temperature and salinity, effluent was expected, but its presence was not then

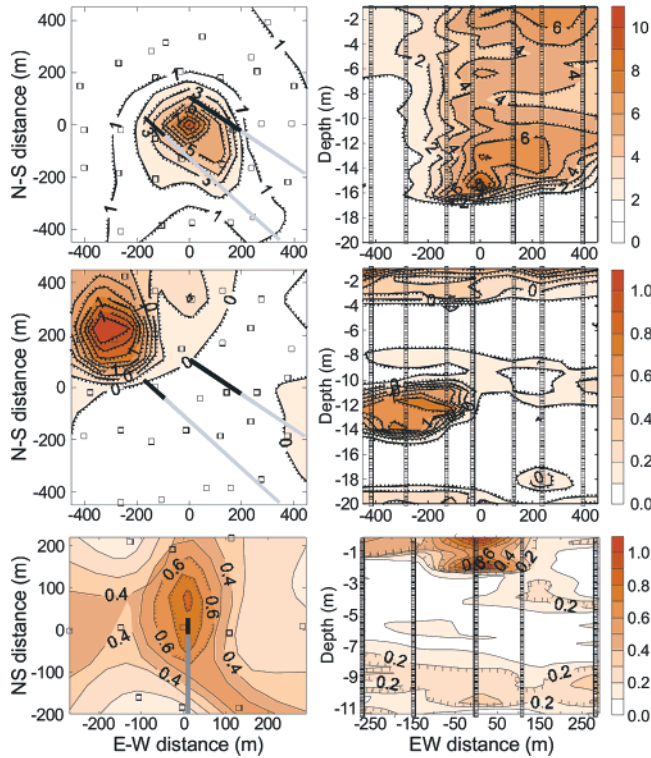


Figure 3. Left: horizontal distribution of l_T at a depth of 16 m on September 26, 1997, above the outfall off Piran (top), at a depth of 13.5 m on October 12, 1998, above the same outfall (middle), and at a depth of 0.2 m on May 10, 2000, above the outfall off Izola (bottom). Dark and gray straight lines mark the diffusers and pipes in a simplified way. Right: vertical distributions of l_T in the E–W direction that cuts through the central station of the near field for the respective cruises. Small rectangles mark the positions where casts were made. The Kriging interpolation procedure was applied, where the grid lines were separated for 112.5 m.

confirmed on board. The water was, therefore, pumped from different depths and samples were analyzed in the laboratory for faecal coliform bacteria.¹³

B. Numerical Model of Initial Dilution. It is supposed that the turbulence of the ambient sea is insignificant compared to the turbulence of the emerging sewage water. This is expected in the larger portion of the uplift cone of sewage above a single orifice of the diffuser, especially in the lower part of the water column throughout the year, while in the upper part, the turbulence imparted by wind may mask the turbulence of the sewage. Another supposition is that the mass and volume fluxes of a discharge are constant during the uplift of a plume. This condition is much easier to meet for the diffusers at Piran, since the time in which the buoyant plume would reach the sea surface or a buoyantly neutral layer is never longer than 1 min and the sewage load does not vary significantly during this time. The numerical model (“SplnRun”) is elsewhere described, studied,² and applied.²⁹ Only a brief summary of equations will be presented here.

The entrainment of ambient fluid through the plume’s side surface³⁰ is the process that controls the dilution in the plume. This means there is a change in the volume flux ϕ along the trajectory $s(t)$ of the plume’s core, which is parametrized in the following way:

$$\frac{d\phi}{ds} = E = 2\pi b\alpha u(s)$$

where b is the radius at which the velocity falls to $1/e$ of the axis value and the plume’s side surface is composed of a perimeter of $2\pi b$ and a height of ds . The peak velocity at the center of a plume’s slice is $u(s)$, and α ($\cong 0.08$) is the entrainment parameter. Gaussian variations of the velocity $u(r,s)$ and of the density deficit $\Delta\rho$ ($= \rho_a - \rho$) across the buoyant slice are supposed to simplify the problem:

$$u(s,r) = u(s) e^{-r^2/b^2} \quad \Delta\rho(s,r) = \Delta\rho(s) e^{-r^2/\lambda^2 b^2}$$

where a second model parameter λ has been introduced and where $\rho_a = 1000.0 + \sigma_T$ is the ambient density with the density excess σ_T . The cross-sectional profile of the density deficit is wider than the profile of velocity ($\lambda \cong 1.2$), which was ascertained experimentally.²² The rate of change of the radial component of the momentum flux is zero, while the vertical component of the momentum flux is controlled by the buoyancy force. The buoyancy flux varies in the stratified ambient ($d\rho_a/dz \neq 0$) and is conserved in the homogeneous ambient. Four equations for the variations of these fluxes along the plume’s path s are expressed in terms of core velocity u , the plume’s radius b , the angle of inclination of a tangent of a plume’s trajectory to the horizontal axis θ , and the core density deficit $\Delta\rho$:

$$\frac{d(ub^2)}{ds} = 2\alpha bu$$

$$\frac{d(u^2 b^2 \cos \theta)}{ds} = 0$$

$$\frac{d(u^2 b^2 \sin \theta)}{ds} = \frac{2g\Delta\rho\lambda^2 b^2}{\rho_{a0}}$$

$$\frac{d(\Delta\rho ub^2)}{ds} = \frac{(1 + \lambda^2)}{\lambda^2} ub^2 \frac{d\rho_a}{ds}$$

where $\rho_{a0} = \rho_a(s = 0)$ is the ambient density near the orifice. This system is transformed into a system of explicit coupled nonlinear equations³¹

$$\frac{du}{ds} = \frac{2g\lambda^2\Delta\rho}{\rho_{a0}u} \sin \theta - \frac{2\alpha u}{b}$$

$$\frac{db}{ds} = 2\alpha - \frac{g\lambda^2\Delta\rho b}{\rho_{a0}u^2} \sin \theta$$

$$\frac{d\theta}{ds} = \frac{2g\lambda^2\Delta\rho}{\rho_{a0}u^2} \cos \theta$$

$$\frac{d\Delta\rho}{ds} = \frac{(1 + \lambda^2)}{\lambda^2} \frac{d\rho_a}{dz} \sin \theta - \frac{2\alpha\Delta\rho}{b}$$

This system was solved²¹ for two specific cases of ambient stratification using the Runge–Kutta method with an adaptive step in the model. This means that the vertical density gradient $d\rho_a/dz$ at an arbitrary height at which there were no measurements of the density ρ_a needs to be known. The density ρ_a and its gradient $d\rho_a/dz$, which vary with the vertical coordinate z ($dz/ds = \sin \theta$), were determined by the cubic

spline interpolation method³² at each step from pairs (z_i, ρ_{ai}) , where ρ_{ai} is the “measured” density at a height of z_i . Additionally, the horizontal distance x of the plume’s core was monitored at each time step ($dx/ds = \cos \theta$) together with the dilution S along the path of the plumes’ center³³

$$S(s) = \frac{4\lambda^2 u(s) b^2(s)}{(1 + \lambda^2)u_0 d^2}$$

Next to the orifice, the source of the pollutant, there is a zone of flow establishment (ZFE)²² in which the core velocity is almost constant along the trajectory and equal to the mean velocity at the orifice [$u(s_0) = u_0 = 4\phi_0/(\pi d^2)$] and the specific momentum flux is conserved. The ZFE is soon over, at a distance of $s_0 = 6.2d$, where d is the diameter of the orifice³¹ and where the zone of established flow (ZEF) starts. At this distance from the orifice, the numerical integration starts. The initial radius of the plume $b_0 = d/2^{1/2}$ follows from the conservation of specific momentum flux ($\pi d^2 u_0^2/4 = u_0^2 \int \exp[-2(r/b)^2] 2\pi r dr$, where the integral goes from zero radius to infinity).² The initial tilt of a buoyant plume is the angle of the inclination of the orifice θ_0 ($= 0$ for the horizontal ejection). The initial density difference $(\Delta\rho)_0$ at $s = s_0$ is expressed with the density difference at the orifice ($\rho_{a0} - \rho_0$), where $\rho_0 = 1000.0 \text{ kg/m}^3$ is the density of an effluent at the orifice: $(\Delta\rho)_0 = (\rho_{a0} - \rho_0)(1 + \lambda^2)/(2\lambda^2)$, meaning that the initial dilution $S_0 = 2\lambda^2/(1 + \lambda^2)$.² The initial position of a plume’s core is $x_0 = s_0 \cos\theta_0$, $z_0 = s_0 \sin\theta_0$.

The model run may be stopped when the density difference $\Delta\rho$ changes sign and the pollutant is passing through the level of neutral buoyancy. However, at that point, the model is not near singularity and can simulate the plume’s further rise due to inertia. The path of a plume’s rise can be followed up to the point where the core velocity u changes sign. Only those results of a simulation that did not have a change in the sign of the core velocity were considered. At that instant, the plume’s radius starts to increase rapidly and the model blows up.

C. Overturning Length Scale. After the rise of the buoyant plumes that emerge from the orifices of a diffuser, the plumes merge and form an initial cloud of diluted sewage in a layer of neutral buoyancy (transition zone). This cloud is thereafter stretched by currents, which is a matter of secondary dilution. However, another property of fluids was applied in getting an impression about the initial patch of a pollutant before it is stretched by ambient currents. There are many cases when fluid parcels do not have a density higher than that of parcels above or lower than that of parcels below, meaning that the density profile is not statically stable. The slight difference in density would drive fluid particles up or down. We may simply sort the parcels so that they have their density increasing with depth. By labeling each particle, we may monitor their vertical displacements and calculate their root-mean square (rms) values (l_T) over suitable depth (height) intervals of size Δz . This method, based on the concept of the “overturning length scale”, was applied to temperature profiles in lakes and seas where salinity does not play a significant role.^{5,18} Although it was applied mainly for shear-generated turbulence, it makes sense also in places where convective overturns occur. In a mixed layer, where the density is homogeneous, the maximum vertical extent of the

potential migration of fluid particles is bounded by the thickness of a mixed layer.

A simple straightforward method for the detection of an effluent was designed on this concept,²¹ by using a standard sorting procedure for the vertical profile of displacements of density parcels that relies on the bubble sort method.³² The density profile $d_i = -h_{Si} + h_i$, where h_i is the original depth of a fluid particle with density σ_{Ti} and h_{Si} is its final depth after sorting. Only those data records were selected for further processing in which the depth (pressure) increased over time during the drop of the probe. It was shown²¹ that, by varying the bin size Δz from 0.1 to 1.0 m, the method gives very similar values for l_T that lead to an indication at which depth the effluent may reside under the sea surface. It is, thus, relatively robust; although, if Δz is too large, details of the turbulence could not be captured. Minimum Δz is determined by the dimension of the conductivity cell ($= 0.11 \text{ m}$), which is placed vertically in the probe. Results for $\Delta z = 0.25 \text{ m}$ will be described.

D. Modeling of Secondary Dilution. Once the patch of pollutant is formed above the diffusers, stratification on its own is not the most important agent for secondary dilution. Stratification of the sea also affects the structure of currents through reduced gravity (gravity in concert with buoyancy); however, many other mechanisms (Coriolis force, friction between layers of fluid, forcing at the sea surface, nonlinear advective accelerations, and pressure gradient force) play significant roles as well. Currents are the agent that may stretch and “shape” the patch rapidly, while horizontal diffusion smears it, usually on a longer time scale. Therefore, it is frequently accepted that “currents” are the agents most responsible for secondary dilution. If currents are known (e.g., from the model) together with the properties of a pollutant, then one may predict the evolution of a patch of pollutant. The most important driving agent at the sea surface in the shallow gulf is wind; tides play a minor role. The riverine inputs are not negligible;²⁶ however, we will not present their influence in this work. Two methods of modeling the spread of pollutants in the secondary dilution phase will be presented. A survey of the first approach will be given, in which the trajectories of the fluid parcels at the sea surface are driven purely by the wind. The second method utilizes a 3D numerical model which gives good insight into the spread of pollutants under steady wind during winter-time.

For the first approach, we reasonably supposed that, in the central part of the gulf, the winds are similar to those that were measured at the coastal stations around it. The most significant wind weather pattern is the passage of a cyclone over the northern Adriatic. This transient wind forcing was applied in the estimate of the secondary dilution of sewage that would spread from the diffuser located in front of the Bay of Koper. A typical synoptic situation was chosen from early October 1999:³⁴ the cyclone that moved over northern Italy (October 3, 1999) first generated a southern wind (Jugo) over the Adriatic Sea, and on the evening of October 4, 1999, an eastern (Bora) wind began. Winds at a 10 m height over the Gulf of Trieste were obtained from the numerical forecast model ALADIN/SI that simulated the weather for the period of October 2–5, 1999. We supposed that there was a release of sewage at the entrance to the Bay of Koper, where there

were intentions to construct a submarine diffuser. The study should reveal what might happen in typical situations.

Previous analyses of wind and current-meter measurements that were performed for the Italian side of the Gulf of Trieste³⁵ were the basis for our estimate of the wind-driven surface currents in the central part of the Gulf of Trieste. The relation between the wind and current speed also follows from the conservation of the stress of momentum at the sea surface.³⁶ We chose the current speed at the sea surface to be 3% of the wind speed, where the effect of the surface waves through the Stokes drift had already been included in this simplistic approximation of the surface current. The Coriolis force deflects surface currents slightly clockwise from the direction of the wind; in simulations, a turn of 25° was assumed.

For the sake of simplicity, a constant flux of sewage was supposed in the simulations during the secondary dilution, which was monitored through the spread of artificial particles. These originated at the location of the potential diffuser in front of the Bay of Koper and were released with a lapse time of 1 h. Along the path of each of the labeled particles, we supposed an exponential decay of bacteria with the decay time $T_{90} = 3.5$ h. This value of decay time is the upper limit of the suggested time interval,³⁷ and we chose it to be on the safe side of the estimate of secondary dilution.

The dispersion of fluid particles is supposed to be governed by two types of dynamics: advection and turbulent diffusion. For advection, we considered surface wind-driven dynamics, where it was supposed that particles in the wind-driven currents are trapped in the surface layer, in order to monitor their largest extent during a typical passage of a cyclone. Artificial particles were tracked with the Lagrangian approach in which the depth-averaged velocities of surrounding numerical cells were spatially interpolated to the positions of the released particles at each time step. In this way, the advective motion of the particles was resolved.

Turbulent diffusion was added to the advective drift of particles at each time step. The velocity field was already calculated from the wind, whereas, for diffusion, a random-walk method was inserted during the integration. Vertical diffusion was ignored since it is much smaller than the horizontal for at least 1 order of magnitude, being quenched by stratification and by boundaries (sea surface and sea floor). Horizontal diffusion was introduced with two independent random number generators R_r and R_φ in the interval [0, 1], the first for the random step Δr and the other for its direction φ :³⁸

$$\Delta r = R_r \sqrt{12K_H \Delta t} \quad \varphi = 2\pi R_\varphi$$

where it is supposed that the coefficient of the horizontal diffusion $K_H = 10$ m²/s is a value that was chosen for the spread of the Po river plume in the northern Adriatic³⁹ under Bora wind conditions. The variance of Δr is $4K_H \Delta t$. Suppose that Δr is a random step in the interval [0, R]; then, one finds $R = (12K_H \Delta t)^{1/2}$ by equating the rms(Δr) = $(4K_H \Delta t)^{1/2}$ with

$$\sqrt{\int_0^R r^2 dr/R}$$

which leads to the above expression for Δr .

The above method, although offering a good approximation for the spread of pollutants in a wind-driven flow, is limited to the surface layer and is not based on the numerical modeling of circulation, which is used in the second method for modeling the spread of pollutants during secondary dilution. The numerical model was recently developed, and from the field of currents, we can obtain an impression regarding the spread of pollutants. The Princeton Ocean Model (POM) was, therefore, installed for circulation studies of the Gulf of Trieste (ACOAST-2), with a horizontal resolution of 0.5 km. Tides were not taken into account in the circulation study, the reasons for which will be addressed in the Discussion. The model is one-way nested in the coarser ASHELF-1 (nesting) model of the larger northern Adriatic area, which has a resolution of 1.5 km. The ASHELF-1 model⁴⁰ was driven in a “perpetual year” mode to capture the climatological circulation of the northern Adriatic. The open-boundary line (OBL) of the ACOAST-2 model coincides with the grid line of the ASHELF-1 model. The grid of ACOAST-2 was generated from the mesh of the ASHELF-1 model by condensing it by a factor of 3.⁴¹ Here, it will be sufficient to point out that, along the vertical, the model has 11 σ layers and that, along the OBL, we applied fluxes of momentum, heat, and salinity, as well as the sea-surface elevation, obtained from the ASHELF-1 model. The OB condition for velocities was corrected at each time step to keep the total flux of mass to zero⁴² in order to conserve the water mass inside the basin. At the sea surface, the model was forced by the wind stress and the solar flux minus the upward heat flux. All were obtained from the European Center for Medium Range Weather Forecasting (ECMWF) with a horizontal resolution of 1.125° and were regridded to the much finer grid of the model. For the depth-averaged velocity, the outward radiation condition was applied.

Since stratification during the winter is weak and the Bora wind field is the dominant forcing agent, simulations were completed for a typical winter situation. Temperature and the salinity field were also initialized with the data of the coarser model, while, during the run, they were passed from the coarser model through the OB plane according to the upstream advection scheme.

RESULTS

A. Initial Dilution. On the windy morning of September 26, 1997, the sea-surface temperature at a depth of 0.5 m was around 20.12 ± 0.05 °C, much higher than the air temperature (13–19 °C). The surface cooling was prolonged from the night into the daytime, causing free convection at the surface to act together with that forced by the wind itself. Salinity varied much less, around 36.7 ± 0.03 PSU. This resulted in a vertically homogeneous surface layer with regard to temperature T , salinity S , and density σ_T down to a depth of 16 m at all 31 stations of the near field.²¹ Therefore, the layer with a sharp vertical density gradient near the sea floor (pycnocline) was governed by the vertical temperature gradient (Figure 4, left).

During the second survey above the diffusers off Piran, conducted on the calm morning of October 12, 1998, the temperature at a depth of 0.5 m was 17.8–19.1 °C. Salinity ranged pronouncedly between 29.5 and 33.3 PSU—a surface layer of fresher water was present. During that period, there

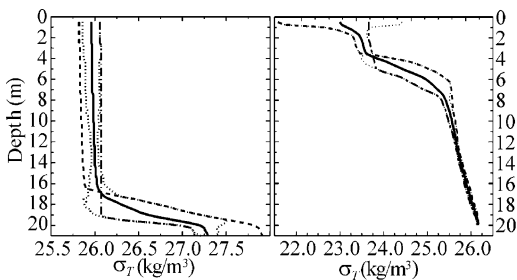


Figure 4. Vertical distribution of the density excess (above 1000 kg/m^3), on September 26, 1997 (left), and on October 12, 1999 (right), averaged over 31 stations of the near field (full line), of averaged values minus 2 standard deviations (SD)s, and averaged values plus 2 SDs (dotted) and the distribution of the sharpened density profile with a sharpened pycnocline (dashed) or a weakened pycnocline (dash-dotted line).

was a lot of riverine freshwater over the northern Adriatic, which manifested at the places of measurement down to depths of 2–8 m. The pycnocline near the sea surface (Figure 4, right) resulted from the vertical gradient of salinity. Temperature increased with depth in the surface layer of fresher water, while in the layer below, it could either increase or decrease with depth, although the density continuously increased. The stability of the water column, however, is not guaranteed,⁴³ since heat has a coefficient of molecular diffusivity ($= 1.5 \times 10^{-3} \text{ cm}^2/\text{s}$) 2 orders of magnitude larger than that of salt, which causes diffusive convection due to faster heat exchange in double diffusion processes, a common phenomenon in the autumn period.⁴⁴ The initial spread of effluent depends pronouncedly upon stratification, and therefore, variations of ambient density during the field campaign have to be taken into account. For this reason, we wanted to capture the least-pronounced stratification, as well as the sharpest one. We composed the least-pronounced stratification by adding 2 SDs (SD = standard deviation) of density to the mean (horizontal average, full lines in Figure 4) in the layers of thickness Δz_L above the pycnocline and subtracting 2 SDs in the layers below it. The sharpest stratification was obtained by subtracting 2 SDs in the layers above the pycnocline and adding 2 SDs in the layers below it (Figure 4, dashed lines). Additional minor modifications of the density profiles provided their statical stability. Since the initial spread of an effluent depends also on the initial discharge velocity u_0 , simulations were performed for $u_0 = 0.39, 0.45,$ and 0.55 m/s for the first survey and $u_0 = 0.6, 0.8,$ and 1.0 m/s for the second survey.

For the situation on September 26, 1997, variations of u_0 did not greatly influence the maximum height of spreading in the case of the sharpened pycnocline. The weakened pycnocline, however, allows the plume to erupt to the sea surface, regardless of the value of u_0 . In a layer of neutral buoyancy ($\Delta\rho = 0$, hatched rectangles on plots of Figure 5), the plume is still rising as a result of inertia, unless the sea surface has been reached already. In reality, after reaching the top of a plume ($u = 0$), the plume falls back toward a depth where $\Delta\rho = 0$,²² where the ambient advection smears this plume with plumes that originate from other orifices. The model cannot reproduce these two processes. The cone radius that is reached by a single plume before it spreads horizontally is between 2 and 5 m, the larger radius related

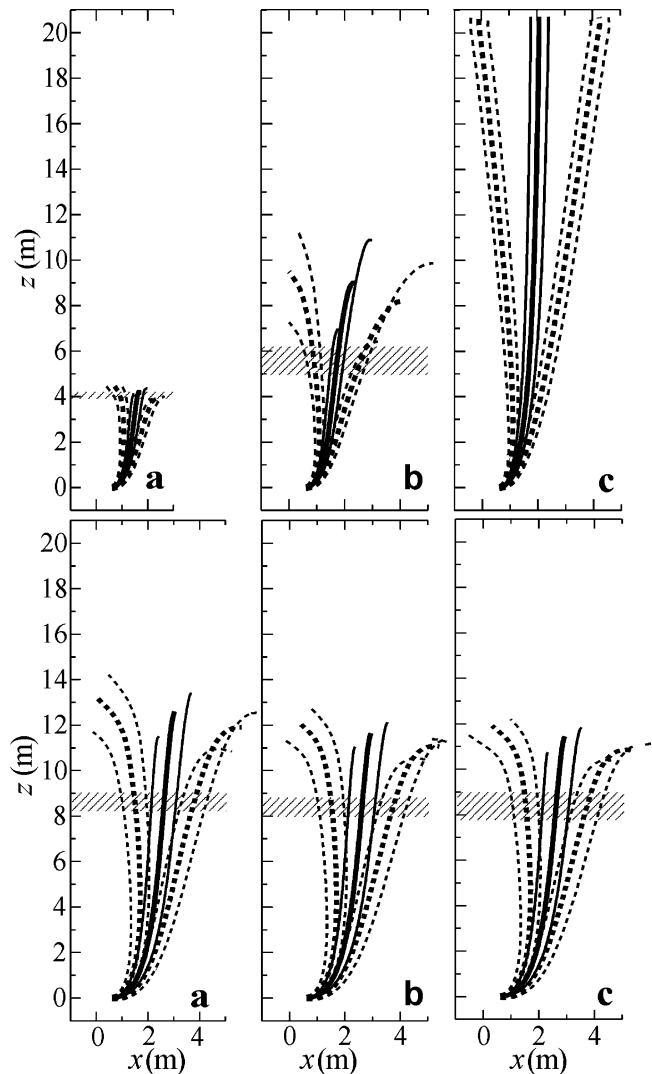


Figure 5. Simulations of a spread of an effluent that emerged horizontally from an orifice of the diffuser on September 26, 1997 (top), and on October 12, 1999 (bottom), when the ambient density profile was (a) that with a sharpened pycnocline, (b) equal to the mean density profile, and (c) that with a weakened pycnocline. Full lines: path of the center of the core of an effluent. Dashed lines: envelopes of an effluent where the concentration is $1/e$ of that in the core's center. Top: the spread with initial velocity at the orifice $u_0 = 0.45$ (thicker lines), $0.36,$ and 0.55 m/s (thinner lines). Bottom: $u_0 = 0.8$ (thicker lines), $0.6,$ and 1.0 m/s (thinner lines). Hatched rectangles mark the area where $\Delta\rho = 0$ for three different values of u_0 .

to the weak pycnocline. We may conclude that the major concentration of an effluent would range between 5 and 7 m above the sea floor for the first survey (Figure 5, top), where the height of the orifice with respect to the sea bed (of about 1 m) is considered, and that the effluent also occupies the space above these heights. This means that peak concentrations of an effluent were located at depths between 14 and 16 m on September, 26, 1997, where the depth of the sea floor is around 21 m. The uncertainty of these depths is on the order of 1 m. The plume's height agrees with the vertical distribution of l_T and faecal coliforms. The dilution factor S varies significantly with stratification, especially when the outflow velocity is small, $u_0 = 0.36 \text{ m/s}$. It ranges between 22 and 354. The initial dilution process is completed in less than 2 min.

There are more possibilities in creating the strongest and the mildest stratifications around the mean profile for the second survey on October, 12, 1998. However, a similar concept of adding and subtracting 2 SDs was applied to the pycnocline at the surface, while care was taken to ensure the increase of the density with depth. Contrary to the previous case, all nine simulations (three initial velocities multiplied by three density profiles) gave similar results (Figure 5, bottom), even with a larger range of initial velocities (0.6, 0.8, and 1 m/s), where the plume was kept below the sea surface at a height of around 9.0 m ($\Delta\rho = 0$). Now, however, the plume heights are the largest for the weakest stratification, since, in this case, there is the largest vertical density gradient in the bottom part of the water column, which matters significantly in the uplift of the sewage. The height at which $\Delta\rho = 0$ lies in the interval between 7.9 and 9.0 m, or at depths between 11.7 and 12.8 m, while the dilution is in a much narrower range, between 63 and 68. In both cases, the maximum radius that individual plumes could reach before merging in a layer of neutral buoyancy are on the order of a few meters.

B. Between Initial and Secondary Dilution. During the first cruise on September, 26, 1997, when the density profile was governed by temperature, one observes that there is roughly a local maximum of the overturning length scale (rms of displacements) near the surface, where displacements are actually negative (downward), and at a depth of 16 m (Figure 6, top), where displacements are positive as a result of convective overturn. However, the peak at a depth of 16 m is larger because of the presence of the alien water that is emerging from the diffusers and this being where a narrow peak of faecal coliform was detected,²¹ just above the sharp pycnocline. This depth also corresponds well to the lowest height of the initial rise (5 m above the diffusers) of effluent that was predicted numerically. In the top right plot of Figure 6, minima of l_T over all 31 stations of the near field are close to zero except for the 4 m near the surface.⁴ The vertical distribution of the average of l_T over 31 stations does not show a significant peak, while maxima of l_T have a peak, again located at a 16 m depth.

On the second cruise on October 12, 1998, several patches of larger displacements were generated by the density profile (governed by salinity), the largest of them expanded between 11 and 14.5 m at the station in front of the left-hand diffuser (Figure 6, middle). The vertical profile of FC (faecal coliforms) now has a much broader peak between 11.0 and 16.7 m, with values larger than or equal to 265/100 mL. However, since the sampling resolution (vertical distance) was poor, we may say that the layer with a larger faecal load begins with a sharp increase from zero at 10.6 m to 265/100 mL at 11.0 m and ends with an abrupt decrease from 365/100 mL at 16 m to 5/100 mL at 18 m.²¹ The vertical profile of l_T roughly follows the profile of bacteria, having a few peaks between 11.0 and 16.7 m. There are some overturning activities in the fresher surface layer down to 4 m and above the sea floor, below depths of 18.5 m. Statistical distribution of l_T (Figure 6, middle right) confirms that, in the surface layer, there is a maximum (at another station) that is larger than the one observed at depths of 11–16 m, where larger values of l_T and FC are located, and where sewage should rise according to the model of initial dilution. The density profile (Figure 6, middle left) shows the presence

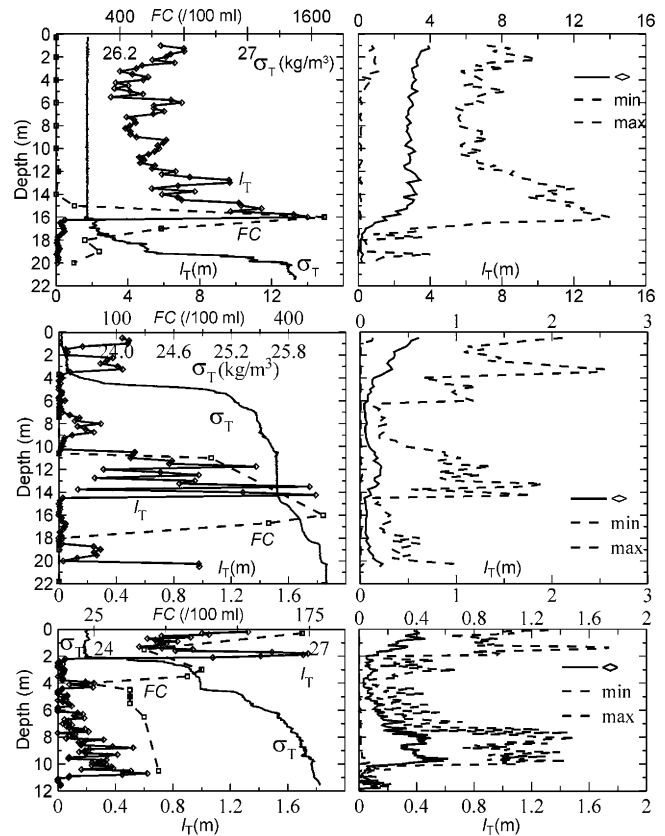


Figure 6. Left: vertical distributions of faecal coliforms (FC, dashed lines), density σ_T (full lines), and overturning length scale l_T (lines with diamonds) at the central station on September 26, 1997, of the near field above the outfall off Piran (top); on October 12, 1998, at the station in front of the left-hand diffuser of the same outfall (middle); and on May 10, 2000, at the central station of the outfall off Izola (bottom). Right: horizontal near-field statistics in layers of 0.25 m (average, minima, and maxima) of l_T for the respective cruises conducted on those dates.

of homogeneous layers of the double diffusion process, which extend just below a small and narrow density spike. A thicker one extends just below a depth of 11.5 m, while two other layers are below 18.0 m, where even more typical figures of the density profile of diffusive convection are evident, similar to those observed in oceans.^{43,45}

The third cruise above the outfall of Izola, which is here described for the first time, was conducted on May, 10, 2000 (Figure 6, bottom plots). Results show that there is a peak of bacteria just below the surface, where l_T has a local maximum. However, another, more-pronounced, maximum is at a depth of 2.0 m, just below the surface mixed layer of fresher water, where density rapidly starts to increase with depth. Statistics from the 11 stations of the near field show that there are quite large maxima of l_T at depths below 8 m. However, detailed inspection shows that the large intensity of turbulence is related to processes in the bottom layer at stations with larger depths (northward from the outfall) and do not correlate with the rise of the effluent, which was emerging to the surface layer in short bursts.

Local peaks of vertical profiles of different quantities lead us to examine the horizontal distribution of l_T (Figure 3, left), especially at depths where local peaks were detected. It has been clearly demonstrated²¹ that, among the horizontal variations of temperature, salinity, density, and l_T , the variations of l_T are the most pronounced and may serve as

an indicator of turbulent alien water. In the central part of the cruise on September 26, 1997, l_T was larger for 1 order of magnitude (10 m) with respect to values at the edge of the near-field zone (1 m). The vertical plane in an E–W direction that passes through the center of the near field (Figure 3, top right) also shows variations of the overturning length scale for 1 order of magnitude. A large underwater plume is formed that extends horizontally and vertically above a depth of 17 m, with a tail, which is 1 m higher than the core (depth 16 m) and spreads eastward. The core is at the depth of the maximum abundance of FC, which is also the lowest height up to which the effluent should rise according to the model. This spread of l_T is in accordance with the most recent numerical simulations of the circulation of the Gulf of Trieste during Bora wind forcing, performed by the POM that is nested in another model of the northern Adriatic Sea,⁴⁶ and with current-meter observations of the coastal oceanographic buoy, less than 2 km away from the diffusers in a northeasterly direction. They show a counter-current at depths during Bora wind episodes.^{41,46} Model results of circulation are presented in the Discussion.

On October 12, 1998, at a depth of 13.5 m, the overturning length scale varies between 0.0 and 1.7 m (SD = 0.32 m, average 0.16 m); the relative change is 100%, for 2 orders of magnitude larger than those of temperature, salinity, and density.

On May 10, 2000, above the outfall off the town of Izola (Figure 3, bottom), it is clear that l_T just below the sea surface is at its highest value around the central station above the small diffuser, which decreases radially outward (Figure 3, bottom left). A vertical E–W cross section shows that this higher intensity is limited to a surface layer of a thickness of 2 m above the diffuser, which decreases with the distance from the center of the near field (Figure 3, bottom right).

C. Secondary Dilution. Wind-Driven Spread of Sewage. In secondary dilution, advection plays a dominant role. Here, a survey of a simulation of the spread of pollutants at the sea surface under nonsteady wind forcing will be presented. For this case, the time series of a surface wind-driven current, which we calculated from the wind data at the sea surface (ALADIN/SI model), was applied. Since we were interested in the spread of pollutants in front of the Bay of Koper, where there was an interest to place an underwater diffuser, we released artificial particles of pollutant at the location of a potential diffuser. We supposed that all particles have the same abundance of bacteria (equal to 1) at the starting point. Over an interval of 3 days, 72 artificial particles were released with a time delay of 1 h, starting on October 2, 1999. Along the path of each particle, the abundance of bacteria exponentially decreases ($T_{90} = 3.5$ h); each particle was monitored for 12 h during 3 days of simulation.³ When all trajectories are plotted together, regardless of their starting time, the isolines of the envelope of bacteria (Figure 7) along all trajectories show the extension of bacteria around the diffuser over 3 days of simulation. This is not the plot of the instantaneous distribution of bacteria. The latter would be much narrower, confined to a few trajectories of particles that were released most recently; the first trajectories would extend toward the north and the last toward the west of the point of release. There are two elongations from the point of release that correspond to the southern and eastern winds. The point of release is almost 4 km westward from the

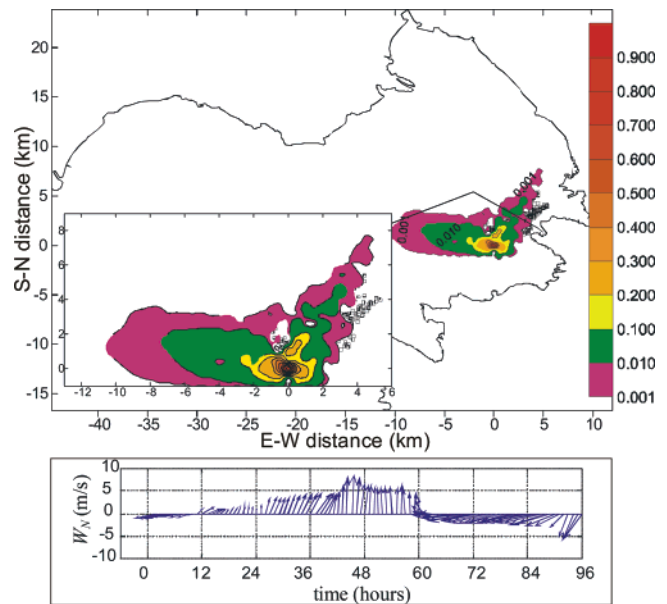


Figure 7. Simulations of a spread of bacteria under windy conditions when a cyclone was passing over the northern Adriatic on October 2, 1999. Top: Isolines represent the envelope of the abundance of bacteria that were released during a 3 day simulation in the wind-driven surface. Trajectories of 72 particles that were continuously released with a delay of 1 h and were observed for 12 h. The number of bacteria is normalized to 1 in the starting position. The straight line that divides the Gulf of Trieste is the borderline between Slovenia and Italy. Bottom: wind vectors of the prognostic model Aladin/SI at the potential location of the diffuser in front of the Bay of Koper (see Figure 1). W_N is the northern component of the wind.

nearest land point. The isoline 0.01 extends northward (in Italian waters) for less than 2 km. Since, from the studies of initial dilution, it is reasonable to suppose that the initial dilution of the potential diffuser at Koper would also be 100 at the sea surface, a total dilution of 10^4 is already achieved inside the patch (the isoline of 0.01), which is a number recommended by UNEP.³⁷

DISCUSSION

The numerical model of initial dilution requires small (negligible) ambient turbulence. Under wind forcing and convective cooling at the surface, this condition is hard to meet. It has been shown in the case of the first cruise of September 26, 1997, that l_T had high values above a depth of 16 m; however, at depths below this limit, l_T had small values and the sewage cones could rise up to the level of neutral buoyancy in a relatively “calm” ambient. There are also, of course, processes near the sea floor (density and turbidity currents⁴⁷). Then, the overturning length scale is affected by the combined action of the ambient turbulence and the turbulence of the alien fluid. The local extreme of l_T does not necessarily mean that an alien fluid is located there. However, if we have a reason to suspect that an alien fluid that emerges in an ambient fluid is turbulent, then it is highly probable that it is located in one of those places where l_T has a local extreme and not where l_T is low.

The application of the distribution of the overturning length scale in the near field of sewage above an outfall is a new approach. However, the formation of the wastewater field above the outfall was studied decades ago,²² and the

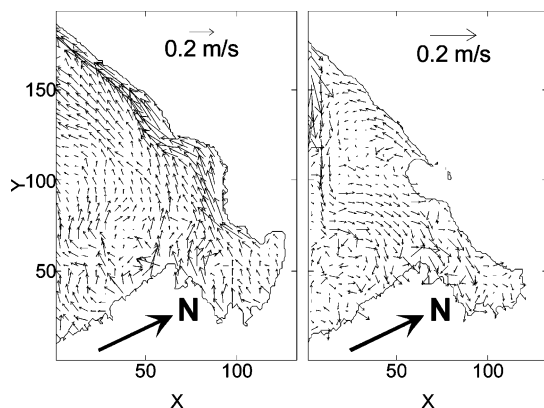


Figure 8. Numerical simulation of climatological circulation in the Gulf of Trieste and its neighborhood during the winter period at 1 and 15 m depths, which was run with the 3D POM. The model is composed of 11 σ layers, and the horizontal resolution of the grid cells is of 0.5 km. Model coordinates are rotated so that the OBL is at the left-hand side of the model domain. Along the OBL, the OB conditions (velocities and elevation) were provided from the coarser model of the northern Adriatic (ASHELF-1). For clarity, only every fifth vector of velocity is presented. Note the general outflow from the gulf in the surface layer and the general inflow at depth. The circulation is dominated by the Bora wind; however, heat fluxes at the surface and the penetration of light have also been accounted for.

analytical expressions for simplified ambient cross flow were then developed. They consider that, when a patch of wastewater is formed inside the water column, the dilution of sewage that is emerging from a single orifice is somehow blocked when it rises toward the bottom of the already existing sewage patch. Unfortunately, these solutions for the thickness of the waste field above the outfall and the correction factor of dilution do not account for the vertical shear of currents nor for density stratification and are, therefore, difficult to apply in real situations.

The presented case of secondary dilution under wind forcing is a good simple view of the circumstance of surface drift. If, however, the effluent spreads vertically through layers of different dynamics, with a pronounced vertical shear between them, the situation looks much more complex. Studies of dispersion in this direction will follow. Recent numerical simulations of circulation in a climatological sense show that advection is quite complex, even when simple driving mechanisms dominate, as in the case of the steady Bora wind which blows along the axis of the Gulf of Trieste and drifts the mass at the surface out from the gulf (Figure 8). It is obvious that, during winter (long-lasting Bora wind), there is a general outflow from the gulf at the sea surface and a balancing inflow at depth. The surface layer of the outflow is not thicker than a few meters in most parts of the gulf. The surface outflow along the southern coastline is deflected across the gulf at its entrance toward the northern coastline, close to which the depths are much shallower and where there is a strip of fresher water mass of river origin (not shown). The Coriolis force is certainly responsible for this deflection, but the balance of forces needs to be examined, as well as the formation of anticyclonic vortices outside the gulf, which complicate the general inflow/outflow scheme. If sewage spreads vertically over the water column and would be released at the southern side of the gulf's entrance (location of the outfall off Piran) during Bora winds, then at the surface it would be drifted out of the gulf, toward

the northern coastline, while at depth, it would flow along the southern coastline in the gulf's interior.

Although the circulation pattern, obtained from the 3D numerical model, is very illustrative, the study of dispersion for this and other circulation cases is not yet completed. A comparison of the model dispersion at the surface with the dispersion in which the advection was approximated as a fraction of a wind speed will be analyzed. In this context, we may point out recent modeling efforts⁴⁸ to show that upwelling of the water mass near the sea floor close to the closed end of the gulf (a few miles off Trieste) is already successfully simulated. Consequently, upwelling significantly affects the dispersion of pollutants. Another driving agent also plays a significant and transient role in the dispersion mechanism: the freshwater runoff that creates density-driven currents, which are out of the scope of this paper.

Model simulations of tides³ showed that, at the location of the potential diffuser at Koper, the mean velocity along the principal axis is only on the order of 10^{-3} m/s, while the standard deviation along it is on the order of 10^{-2} m/s. Within a period of 3 days, particles can be displaced by tides for a few kilometers from the point of release, since the amplitude of tidal currents is on the order of 0.1 m/s. This estimate of the amplitude follows from the conservation of the volume of water mass inside the gulf:²⁷ $A \, dh/dt = \langle v \rangle S$, where A is the depth average mean area of the horizontal plane ($= 590 \times 10^6 \text{ m}^2$), S is the area of the vertical plane across the gulf's entrance ($= 3 \times 10^5 \text{ m}^2$), $\langle v \rangle$ is the velocity averaged over S , and h is the amplitude of the elevation ($= 1 \text{ m}$). We take for the period of tides 12 h (semidiurnal constituents are dominant). However, even if the spread of pollutants would be up to a few kilometers, it is about 1 order of magnitude smaller than that of the wind-driven circulation. This also justifies why tides have not been included in the 3D numerical model of the circulation of the gulf.

CONCLUSION

In this paper, a survey of processes related to the initial and secondary dilutions of pollutants was presented together with a description of a patch of pollutants between these two dilution processes. The position of one of the local peaks of the overturning length scale in the core of a sewage near field matches with the height of the simulated plume rise, as well as with the position of the peak of the vertical distribution of faecal coliforms. It is shown that the calculation of the overturning length scale is a useful technique for operations on-board a vessel since it is easy to implement right after the CTD casts. It enables the detection of turbulent water masses of different origins in lakes, reservoirs, and coastal seas. Although the process of secondary dilution was presented briefly, we may conclude that sewage released in the Gulf of Trieste at points that are a few miles off-shore reach a factor of total dilution of 10^4 , when, in the secondary dilution, the decay of bacteria is taken into consideration.

A new understanding of the circulation in the gulf during the Bora wind in winter, which results from the numerical simulations, gives an idea about the distribution of a pollutant during the secondary phase of dilution. In the southern part of the gulf, circulation stretches the patch of a pollutant at the sea surface out of the gulf, while the patch at depth is elongated and parallel to the coastline and then spreads to

the gulf's interior. New studies of dispersion are on their way, which would take into consideration the complex dynamics of the circulation under different forcing mechanisms.

ACKNOWLEDGMENT

This work was supported by the Ministry of Higher Education, Science and Technology of Slovenia, by the Municipality of Izola, and by the Italian Ministry of the Environment through the ADRICOSM project (INGV in Bologna). Boris Petelin prepared the results of the numerical modeling of the circulation during the Bora wind.

REFERENCES AND NOTES

- Lewis, R. *Dispersion in Estuaries and Coastal Waters*; John Wiley & Sons: Chichester, U. K., 1997.
- Malačič, V. Numerical modelling of the initial spread of sewage from diffusers in the Bay of Piran (northern Adriatic). *Ecol. Modell.* **2001**, *138*, 173–191.
- Malačič, V.; Petelin, B.; Vukovič, A.; Potočnik, B. Municipal discharges along the Slovenian littoral (the northern Adriatic Sea) – community planning and the environmental load. *Period. Biol.* **2000**, *102*, 91–100.
- The acquisition, calibration, and analysis of CTD data. A report of SCOR Working Group 51*. UNESCO: Paris, 1988.
- Dillon, M. T. Vertical overturns: A comparison of Thorpe and Ozmidov length scales. *J. Geophys. Res.* **1982**, *87*, 9601–9613.
- Oakey, N. S.; Elliott, J. A. Dissipation within the surface mixed layer. *J. Phys. Oceanogr.* **1982**, *12*, 171–185.
- D'Asaro, E. A.; Dairiki, G. T. Turbulence intensity measurements in a wind-driven mixed layer. *J. Phys. Oceanogr.* **1997**, *27*, 2009–2022.
- Etamad-Shahidi, A.; Imberger, J. Anatomy of turbulence in thermally stratified lakes. *Limnol. Oceanogr.* **2001**, *46*, 1158–1170.
- Fer, I.; Lemmin, U.; Thorpe, S. A. Contributions of entrainment and vertical plumes to the winter cascading of cold shelf waters in a deep lake. *Limnol. Oceanogr.* **2002**, *47*, 576–580.
- Brubaker, J. M. Similarity structure in the convective boundary layer of a lake. *Nature* **1987**, *330*, 742–745.
- Imberger, J.; Hamblin, P. F. Dynamics of lakes, reservoirs, and cooling ponds. *Annu. Rev. Fluid Mech.* **1982**, *14*, 153–187.
- Thorpe, S. A. Dynamical processes of transfer at the sea surface. *Prog. Oceanogr.* **1995**, *35*, 315–351.
- Mozetič, P.; Malačič, V.; Turk, V. Ecological characteristics of seawater influenced by sewage outfall. *Annales* **1999**, *9*, 177–190.
- Malačič, V.; Vukovič, A. Preliminary results of the submarine outfall survey near Piran (northern Adriatic Sea); *Tracer Hydrology 97*; Kranjc, A., Ed.; Balkema: Portorož, Slovenia, 1997; pp 263–268.
- Petrenko, A. A.; Jones, B. H.; Dickey, T. D. Shape and initial dilution of Sand Island, Hawaii sewage plume. *J. Hydraul. Eng.* **1998**, *124*, 565–571.
- Washburn, L.; Jones, B. H.; Bratkovich, A.; Dickey, T. D.; Chen, M.-S. Mixing, dispersion and resuspension in vicinity of ocean wastewater plume. *J. Hydraul. Eng.* **1992**, *118*, 38–58.
- Sherwin, T. J.; Jonas, P. J. The impact of ambient stratification on marine outfall studies in British waters. *Mar. Pollut. Bull.* **1994**, *28*, 527–533.
- Thorpe, S. A. Turbulence and mixing in a Scottish Loch. *Philos. Trans. R. Soc. London* **1977**, *286*, 17–181.
- Flór, J. B.; Fernando, H. J. S.; van Heijst, G. J. F. The evolution of an isolated turbulent region in a two-layer fluid. *Phys. Fluids* **1994**, *6*, 287–296.
- Fonseka, S. V.; Fernando, H. J. S.; van Heijst, G. J. F. Evolution of an isolated turbulent region in a stratified fluid. *J. Geophys. Res.* **1998**, *103*, 24857–24868.
- Malačič, V. Initial spread of an effluent and the overturning length scale near an underwater source in the northern Adriatic. *J. Mar. Syst.* **2005**, *55*, 47–66.
- Fischer, H. B.; List, E. J.; Koch, R. C. Y.; Imberger, J.; Brooks, N. H. *Mixing in Inland and Coastal Waters*; Academic Press: New York, 1979.
- Olivotti, R.; Faganeli, J.; Malej, A. Impact of 'organic' pollutants on coastal waters, Gulf of Trieste. *Water Sci. Technol.* **1986**, *18*, 57–86.
- Ogrin, D. *Climate of Slovenian Istra*; Zgodovinsko društvo za Južno Primorsko (In Slov): Koper, Slovenia, 1995.
- Malačič, V.; Viezzoli, D.; Cushman-Roisin, B. Tidal dynamics in the northern Adriatic Sea. *J. Geophys. Res.* **2000**, *105*, 26265–26280.
- Malačič, V.; Petelin, B. Gulf of Trieste. *Physical Oceanography of the Adriatic Sea, Past, Present and Future*; Cushman-Roisin, B., Gačić, M., Poulain, P.-M., Artegiani, A., Eds.; Kluwer Academic Press: Dordrecht, The Netherlands, 2001; pp 167–177.
- Malačič, V.; Viezzoli, D. Tides in the northern Adriatic Sea – the Gulf of Trieste. *Nuovo Cimento* **2000**, *23*, 365–382.
- Lewis, D. P. *A Field Measurement System for Mixing and Biological Investigations*. Centre for Water Research, University of Western Australia; Crawley, Western Australia, Australia, 1992.
- Malačič, V. Rise of effluent from an underwater sewage diffuser in the southern part of the Gulf of Trieste (northern Adriatic) during the bora event. *Rapp. Comm. int. Mer Médit.*; Briand, F., Ed.; CIESM (Commission Internationale pour l'Exploration Scientifique de la mer Méditerranée): Barcelona, Spain, 2004; Vol. 37, pp 121–121.
- Turner, J. S. Turbulent entrainment: the development of the entrainment assumption, and its application to geophysical flows. *J. Fluid Mech.* **1986**, *173*, 431–471.
- Featherstone, R. E. Mathematical models of the discharge of wastewater into a marine environment. *An Introductory to Water Quality Modelling*; James, A., Ed.; John Wiley: Chichester, U. K., 1984; pp 150–162.
- Press, W. H.; Teukolsky, S. A.; Vetterling, W. T.; Flannery, B. P. *Numerical Recipes in Fortran*, 2nd ed.; Cambridge University Press: Cambridge, MA, 1992.
- Fan, L. N.; Brooks, N. H. Horizontal jets in stagnant fluid of other density. *J. Hydraul. Div., Am. Soc. Civ. Eng.* **1966**, *92*, 423–429.
- Vrhovec, T. A few periods of intensive precipitations MAP SOP (In Slov.); *Proceedings of Fifth Assembly of Slovenian Union of Geodesy and Geophysics*; Slovenian Union of Geodesy and Geophysics: Ljubljana, Slovenia, 1999; Vol. 2, pp 50–60.
- Mosetti, F.; Mosetti, P. Measurements on wind driven circulation in the north Adriatic Sea. *Boll. Oceanol. Teor. Appl.* **1990**, *8*, 251–261.
- Csanady, G. T. *Circulation in the Coastal Ocean*; D. Reidel: Dordrecht, The Netherlands, 1982.
- Guidelines for Submarine Outfall Structures for Mediterranean Small and Medium-Sized Coastal Communities. Working document*; UNEP-(OCA): Paris, 1995.
- Al-Rabeh, A. H.; Cekirge, H. M.; Gunay, N. A stochastic simulation model of oil spill fate and transport. *Appl. Math. Modell.* **1989**, *13*, 322–329.
- Kuzmič, M. Exploring the effects of bura over the northern Adriatic: CZCS imagery and a mathematical model prediction. *Int. J. Remote Sensing* **1991**, *12*, 207–214.
- Zavatarelli, M.; Pinardi, N. The Adriatic Sea modelling system: a nested approach. *Ann. Geophys.* **2003**, *21*, 345–364.
- Malačič, V.; Petelin, B. Winter circulation of the Gulf of Trieste (northern Adriatic). *Acta Adriatica* **2005**, in press.
- Marchesiello, P.; McWilliams, J. C.; Shchepetkin, A. Open boundary conditions for long-term integration of regional oceanic models. *Ocean Modell.* **2001**, *3*, 1–20.
- Turner, J. S. *Buoyancy Effects in Fluids*; Cambridge University Press: London, 1973.
- Malačič, V. Estimation of the vertical eddy diffusion coefficient of heat in the Gulf of Trieste (Northern Adriatic). *Oceanol. Acta* **1991**, *14*, 23–32.
- Monin, A. S.; Ozmidov, R. V. *Turbulence in the Ocean*; D. Reidel Publishing Company: Dordrecht, The Netherlands, 1985.
- Malačič, V.; Petelin, B.; Cermelj, B. *Adriatic Sea integrated coastal areas and river basin management system pilot project (ADRICOSM)*; Final Sci. Report, October 2001–September 2004; National Institute of Biology, Marine Biology Station: Ljubljana, Slovenia, 2004.
- Komar, P. D. *In The Sea*; Goldberg, E. D., McCave, I. N., O'Brien, J. J., Steele, J. H., Eds.; John Wiley and Sons: New York, 1977; Vol. 6, pp 603–621.
- Crise, A.; Cavazzon, F.; Malačič, V.; Querin, S. Circolazione indotta dal vento di bora nel Golfo di Trieste: studio numerico in condizioni di stratificazione. *La Difesa Idraulica del Territorio 2003*; Caroni, E., Ed.; Università degli studi di Trieste: Trieste, Italy, 2003, pp 663–677.